Sedimentation / Steric Field-Flow Fractionation: A Powerful Technique for Obtaining Particle Size Distribution

Myeong Hee Moon,[1] Seungho Lee[2]
[1]*Department of Chemistry, Kangnung National University, Kangnung 210-702, Korea*
[2]*Department of Chemistry, Hannam University, Daejon 300-791, Korea*

Received 30 December 1996; accepted 21 January 1997

Abstract: This review provides a brief overview of particle size characterization by Sedimentation/ Steric Field-Flow Fractionation (Sd/St FFF) and discusses the retention in steric FFF, the recent findings on hydrodynamic lift forces, and the density compensation calibration procedure for obtaining size distribution of supramicron-sized particles. A number of applications to the determination of particle size distribution are discussed with some practical considerations such as steric inversion diameter, size selectivity, and selection of an optimum calibration run condition. *J Micro Sep* **9:** 565–570, 1997

Key words: *sedimentation / steric field-flow fractionation; particle size distribution; separation of particles; density compensation calibration procedure*

INTRODUCTION

Sedimentation/ steric field-flow fractionation (Sd/StFFF) has been developed into a high-speed and powerful technique for the separation and size determination of particulate materials in the size range 0.3 to ~ 100 μm [1–6]. Like other FFF techniques, separation in Sd/StFFF is carried out in a thin flow channel under an applied field directing perpendicular to the channel flow. The type of force applied to the particles in sedimentation FFF (SdFFF) is a centrifugal acceleration generated by rotating the circular channel. The external field drives particles to move toward the outer wall. In the normal mode of SdFFF (Figure 1a) particles tend to diffuse away from the wall against the external field, and eventually form an equilibrium layer adjacent to the outer wall. The retention mechanism in the normal operating mode of SdFFF is well understood [6–15], and therefore, sedimentation/normal FFF provides accurate particle size and size distributions from the experimental fractogram by theory [9, 10].

As the particle size increases (usually over 1 μm in diameter), the diffusion becomes insignificant, and particles move all the way to the outer wall by the external field. Thus, the protrusion of particles out into the flowstream is determined by the particle size itself rather than Brownian motion [5, 6]. In this case, particle size is the determining factor in the migration velocity of the particle down the channel. Larger particles experience faster flow streams, and thus elute earlier than small ones, resulting in an elution order opposite that of the normal FFF [16], as shown in Figure 1b.

In simple steric FFF theory, particles migrate along the channel in physical contact with the accumulation wall under the applied field force. As particles are forced to move close to the accumulation wall of the channel by the external field, they start experiencing opposing forces (hydrodynamic lift forces) acting against the field force [17–21]. Eventually particles reach an equilibrium position at an elevated distance from the accumulation wall where these two opposing forces are balanced (Figure 1b). Thus, particles migrate faster than would be expected by simple steric FFF theory. Although hydrodynamic lift forces have been vastly studied, their theory has not been clearly revealed yet, owing to the complicated nature of the lift phenomena. A calibration is therefore needed to obtain the particle diameter using Sd/StFFF.

In memory of the late Professor J. Calvin Giddings, this short review discusses some recent findings on Sd/StFFF. Development of the density compensation calibration and its application to the de-

---

Myeong Hee Moon obtained a Ph.D. under the supervision of Cal Giddings in 1991. Seungho Lee obtained a Ph.D. under the supervision of Cal Giddings in 1988.

Correspondence to: M. H. Moon

Contract grant sponsor: Korea Science and Engineering Foundation; Contract number 951-0304-023.

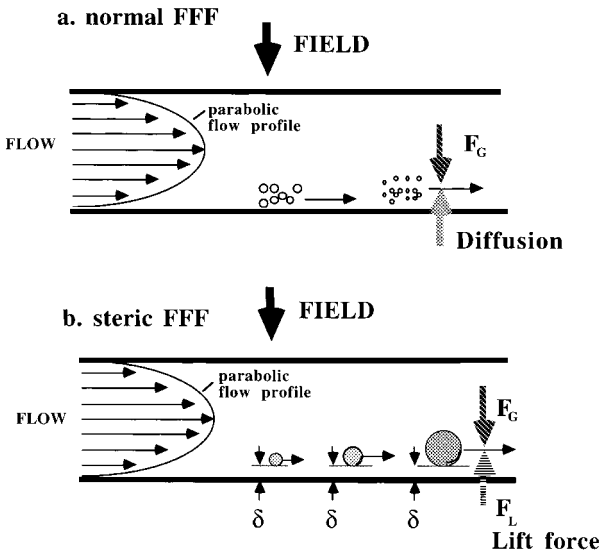

Figure 1. *Schematic view of particle positions and differential particle displacement in (a) normal FFF and (b) steric FFF under sedimentation force F_G.*

termination of particle size distribution of various supramicron-sized particulate materials are described. Practical aspects in using the density compensation calibration method along with some experimental guidelines are also discussed.

STERIC FFF AND HYDRODYNAMIC LIFT FORCES

The retention mechanism of particles in steric FFF is not fully understood using simple theory, because of the complicated role of the hydrodynamic lift forces. However, earlier studies suggest that the retention ratio, the ratio of channel void time t^0 to retention time t_r of a particle [6], in steric FFF can be expressed as

$$R = \frac{t^0}{t_r} = \frac{3\gamma d}{w} \tag{1}$$

where d is the particle diameter, w is the channel thickness, and γ is the steric correction factor originated from the interplay of lift phenomena. The correction factor has been found to increase with the channel flow velocity, and to decrease with an increase of the field strength and particle diameter [22]. According to Equation 1, it is shown that prediction of particle retention in steric FFF requires a clear understanding of the correction factor, γ. Efforts to elucidate the retention mechanism in steric FFF focus on the investigation of the lift phenomena observed for particles under the sedimentation force.

In Sd/StFFF, a particle of diameter d experiences the sedimentation force, F_G, [6] as

$$F_G = \frac{1}{6}\pi d^3 G \Delta\rho \tag{2}$$

where G is the centrifugal acceleration as the product of channel radius and square of rotation rate (G = radius $\times$ rpm^2) and $\Delta\rho$ is the density difference between the particle and the carrier liquid. Under the influence of the sedimentation force, a particle is driven toward the accumulation wall. At the same time, the particle is forced to move away from the accumulation wall in a direction opposite to the sedimentation force. The final position is where the sedimentation force F_G exerting on a particle exactly counterbalances the lift force F_L [18, 19].

Systematic approaches have been made to characterize the hydrodynamic lift forces to better understand the retention behavior in Sd/StFFF. Recent studies [5, 18–21] have shown that the lift forces may be composed of two different contributors: lift force due to the fluid inertial effect and lift force by a near-wall effect. By measuring retention times of well-characterized latex beads 2–50 μm in diameter, and then by equating the field-induced force to the lift force, an empirical lift force equation was obtained [18]. Lift force by the near-wall contribution was experimentally found to be a function of particle radius a, the distance of the particle from the wall, fluid shear rate s_0, and the fluid viscosity η as

$$F_{L_w} = C\frac{a^3\eta s_0}{\delta} \tag{3}$$

where δ is the distance of the particle's bottom from the wall represented in Figure 1b, and C is a dimensionless coefficient. The subscript w in F_{L_w} was added to indicate that Equation 3 is the near-wall contribution to lift force. Under a fixed experimental condition, the lift forces increase with increasing particle size.

Similar efforts were made using lower external field strengths to characterize the lift forces at distance from the wall, the fluid inertial contribution of lift forces [19]. Observed inertial lift forces were in reasonable agreement with values predicted by the inertial lift force theory expressed by

$$F_{L_i} = 13.5\pi\frac{\langle v\rangle^2 a^4 \rho}{w^2} g(x/w) \tag{4}$$

where $\langle v\rangle$ is the mean carrier flow velocity, ρ carrier fluid density, w channel thickness, and $g(x/w)$

is a function of function of (x/w) [5]. The subscript i in F_{L_i} was added to indicate that Equation 4 is the inertial contribution to lift force. Since the lift force is considered to be the sum of fluid inertial and near-wall contributions, a general expression of lift force is obtained by combining Equations 3 and 4 [19]

$$F_L = C\frac{a^3\eta s_0}{\delta} + 13.5\pi\frac{\langle v\rangle^2 a^4\rho}{w^2}g(x/w) \qquad (5)$$

The first term is the near-wall contribution, and the second term is the inertial contribution to the lift force. When particles are near the channel wall, the first term dominates, and when particles are at distance from the wall, the second term dominates.

As briefly explained thus far, much progress has been made to better understand lift forces and their influence on the retention of particles in Sd/StFFF. However, it is not still clear in theory and further studies are needed to account for the unknown characteristics involved in particle migration. A complete understanding of the lift force will lead to a development of theory that explains the relationship between particle size and retention time in Sd/StFFF. It will also allow an accurate prediction of retention time for a known particle size or an accurate determination of particle size from the retention time without the need of calibration as in normal mode of SdFFF. Until then, calibration is still required in Sd/StFFF, and a proper calibration method [2] must be understood.

STERIC CALIBRATION PROCEDURE AND PARTICLE SIZE DISTRIBUTION

In Sd/StFFF, particles injected into rotating channel experience a sedimentation force which is dependent on particle size, centrifugal acceleration, and the density difference according to Equation 1. Thus, particles of different kinds will experience different field forces from their difference in densities. This makes it difficult to use a simple diameter-based calibration method if the density of standards is different from that of sample materials. Here, a proper calibration method needs to be used to incorporate the effect of field forces according to the difference in their densities.

The approach to a needed calibration in Sd/StFFF is started with a density compensation principle [2] in which particles of an identical diameter but different densities can be eluted at the same retention time by adjusting field strengths in such a way as to compensate the density difference between the particles. This idea was practically applied to the size calculation of glass beads with polystyrene latex particles as a calibration standard and the results were confirmed by microscopic examination of narrow particle fractions collected at the end of an FFF run [2].

The underlying principle is based on the following relationship of particle diameter and effective field forces. If the product $G\Delta\rho$ in Equation 2 can be kept constant for two different kinds of particles of an identical diameter, they will experience the same effective force, and thus occupy an equivalent equilibrium position against the bottom wall and elute at the same retention time [2, 6]. This can be done by adjusting the field strength of a sample run inversely proportional to the change in density difference. Practically, the isoretention of two different kinds of particles can be obtained by running an unknown sample at an adjusted rotation rate (or field strength), which is calculated from the established run condition of a standard calibration as

$$(\text{rpm})_{\text{sample}} = \left\{\frac{\Delta\rho_{\text{std}}}{\Delta\rho_{\text{sample}}}\right\}^{1/2}(\text{rpm})_{\text{std}} \qquad (6)$$

where $(\text{rpm})_{\text{sample}}$ represents the rotation rate of an unknown sample run, $(\text{rpm})_{\text{std}}$ is the standard run, $\Delta\rho_{\text{std}}$ is the density difference between the standards and carrier liquid, and $\Delta\rho_{\text{sample}}$ is the difference between the sample and carrier. By means of a carefully chosen adjustment in field strength or rpm using the density compensation principle, it is possible to use any convenient particle standard regardless of the density.

This procedure requires a calibration run using a series of standards (normally done with polystyrene latex standards), which takes only a few minutes. From the observed retention time data of a series of standard particles, a plot of $\log t_r$ retention time, versus $\text{Log}\, d$ can be established, and this plot normally yields a straight line. This relationship, which is well understood using the concept of selectivity [2], is expressed by

$$\log t_r = -S_d \log d + \log t_{r1} \qquad (7)$$

where S_d is diameter-based selectivity, which is typically around 0.7–0.8 [2, 23], and t_{r1} is a constant equal to the extrapolated value of retention time for particles of unit diameter. By using the calibration parameters S_d and t_{r1}, particle size distribution, $m(d)$, which expresses the relative mass, m, of particulate matter in a given diameter scale, can be obtained as

$$m(d) = c(t_r)\dot{V}\left|\frac{dt_r}{dd}\right| = c(t_r)\dot{V}S_d t_{r1}\left(\frac{t_r}{t_{r1}}\right)^{(S_d+1)/S_d} \qquad (8)$$

where $c(t_r)$ is the fractogram signal at retention time t_r and $\dot{V}$ is the flow rate through the channel. To resolve the unknown sample particles into their full size range in Sd/StFFF, selection of an appropriate field strength for the calibration run is very important for the successful fractionation of the sample of a broad size distribution. In practice, it is desirable to scan sample particles first from a low field strength to a higher level. This will minimize the possibility of contaminating the channel by sample adhesion at the channel wall. Then one can establish a calibration run condition whose field strength is equivalent to that of the sample run using Equation 6 in the opposite way.

APPLICATION OF Sd/StFFF FOR PARTICLE SIZE DISTRIBUTION

After the initial evaluation of the density compensation calibration method in Sd/StFFF with the NIST glass bead standards [2], various particulate materials were applied to this technique for characterization of the particle size distribution. Porous silica particles used as chromatographic supports were studied to obtain porosity and density distribution as well as particle size distribution by Sd/StFFF [23]. A novel approach was made to separate submicron metal particles in steric FFF by using gold, silver, copper, and palladium [4, 6]. Since these particles have large densities, they will experience a relatively high force in a sedimentation FFF channel, according to Equation 2. In this case, steric transition diameter d_i was extended into a low submicrometer size by applying a high field strength and flow rate. An empirical equation [4] for calculating steric transition diameter was developed using basic FFF theory jointed with calibration parameters as

$$d_i = \left(\frac{108kTt_{r1}}{\pi G \Delta \rho w t^0 S_d} \right)^{1/(S_d+3)} \quad (9)$$

where kT is the thermal energy. Equation 9 indicates that the steric transition diameter can be lowered by increasing the product $G\Delta\rho$ at a given flow rate. In the case of gold particles with a density of 19.2 g/mL, the steric transition diameter d_i was greatly reduced to ~ 0.2 μm, which was predicted by Equation 9 and confirmed by electron microscopy. To offset the increased retention caused by a strong field, channel thickness and breadth were reduced to half the conventional channel dimension (breadth $b = 2$ cm, $w = 254$ μm), and a very high flow rate (24 mL/min) was used. A series of calibration run conditions with the calculated d_i are listed in Table I, including the case of gold particles in condition *a*. Table I shows the variation of steric inversion points according to the run conditions selected for calibration. This will be discussed later.

Sedimentation/Steric FFF also demonstrated its capability in the size characterization of a series of starch granules [24] such as wheat, corn, and oats, in a relatively high speed (within 5 min of an FFF run). Starch granule size distribution is a contributing factor in the quality of industrial starch products used in adhesives, food, and the paper industries, but their size determination has generally been car-

Table I. *Experimental conditions used for calibration and predicted steric inversion diameters.*[a]

rpm	$\dot{V}$ (mL/min)	$G\Delta\rho \times 10^{-4}$ (g/s^2 cm^2)	S_d	t_{r1} (min)[b]	cc[c]	d_i^d (μm)
a 1120	24.0	378.0	0.795	4.19	0.995	0.21
b 421	29.4	23.19	0.686	1.94	0.991	0.39
c 2300	29.4	4.380	1.062	1.51	0.996	0.60
d 2200	14.5	4.007	0.704	3.56	0.998	0.59
e 1940	15.0	3.116	0.802	4.27	0.998	0.65
f 1800	8.3	2.683	0.781	8.11	0.999	0.69
g 1800	12.8	2.683	0.829	5.81	0.999	0.70
h 1500	6.0	1.863	0.729	8.13	1.000	0.71
i 1400	6.15	1.623	0.727	7.70	1.000	0.73
j 1100	6.0	1.002	0.729	7.43	1.000	0.82
k 1100	10.0	1.002	0.852	5.35	0.997	0.83

[a]The calibrants used are polystyrene latex standards ($\rho = 1.05$ g/cm^3) except for following runs: *a* gold ($\rho = 19.2$ g/cm^3) and *b* copper particles ($\rho = 8.9$ g/cm^3). Channel dimension used is $90 \times 1 \times 0.0127$ cm.
[b]Interpolated retention time of unit diameter (μm).
[c]Correlation coefficient of the regression.
[d]Calculated based on Equation 9.

ried out by microscopy or an image analysis technique, which require laborious work and high cost, respectively. Compared to these techniques, Sd/StFFF provided particle size distributions as well as number distributions of various starch granules in a simple and accurate way. Size characterization of a series of starch granules was accomplished in a channel of the reduced dimension described above. More applications were made to various particle samples such as alumina, low-porosity PVC latex [3], quartz [25] etc. Among these particles, quartz samples (BCR standards 67 and 70) were nonspherical. Since the density calibration principle is valid for spherical particles, it was difficult to obtain accurate size distributions for particles of irregular shape. Owing to the complicated role of hydrodynamic lift forces on nonspherical particles, the calculated particle diameter from a typical PS calibration was less than the equivalent spherical diameter of a relatively flat quartz particle. The entire size distribution of quartz particles obtained by Sd/StFFF appeared to shift to a large-diameter scale compared to the certified data provided by BCR. These features were attributed to the elevated migration of nonspherical particles, which leads to early elution in Sd/StFFF owing to the unknown factors in lift forces. An empirical approximation to correct the apparent size distribution was made to obtain a correction factor of 2.7 for the relatively flat quartz samples [25]. Similar observations in retention perturbation were obtained with cylindrical particles such as glass rods and disc-shaped PS particles, but were reported with different correction factors for accurate particle sizes. An essential part in understanding these unexpected phenomena for nonspherical particles is a well-characterized model for hydrodynamic lift forces which need to be further evaluated.

PRACTICAL CONSIDERATIONS IN THE CALIBRATION PROCESS

The calibration curve, expressed as $\log t_r$ versus $\text{Log}\, d$ in Equation 7, is found to be approximately linear over a substantial diameter range for typical polystyrene latex standards. When the calibration curve extends into the range of smaller particles, it tends to bend down toward shorter retention [2]. This is due to the increasing role of Brownian motion as particle size becomes smaller (< 3 μm). Below this size, particles elute earlier than is expected from the linear calibration curve. Eventually the calibration curve passes a steric inversion point, the transition diameter between steric and normal mode operation typically around 1 μm. As explained earlier, the steric transition diameter can be lowered by applying a high field strength and flow rate in Sd/StFFF. Some of the experimental conditions of calibration runs are listed in Table I obtained by using the reduced channel ($b = 1$ cm, $w = 127$ μm). The run conditions in Table I are listed in increasing order of steric inversion diameter, calculated by Equation 9. The calibrating materials used are mostly polystyrene latex standards except (a) with gold and (b) with copper particles. For the run conditions *c–e*, steric transition diameter can be substantially reduced to 0.6 μm by simultaneously applying a high field strength and high flow rate. The size limit that can be completely resolved by listed run conditions *f–k* is approximately up to 30–40 μm for 2 μm.

On the other end of calibration curve extending into the large-diameter range, the calibration curve starts bending up toward longer retention [26]. When the particle size approaches a substantial fraction of the thickness of an FFF channel, the linear calibration is found to be applicable only for d/w ratios at most 0.3. Since there is a physical limitation of particle sizes that can be accommodated in a given channel, one needs to consider the maximum particle size that can be used for the purpose of calibration. Retention time is observed to depart from linearity in a calibration curve as particle size becomes larger. In case of a reduced channel, linearity has been shown to be valid for particles up to 30 μm. This is due to the lag effect of large particles, related to the channel thickness. When the calibration is obtained by using a regular channel thickness ($w = 254$ μm), the departure from linearity is found to extend as large as 60 μm, except for the slight deviation from the linearity. Although there are size limitations in the linearity of calibration curve, it does not rule out the possibility of calibration, and much larger particles up to a d/w ratio approaching 0.5 could still be separated. However, under severe run conditions such as a high field strength with a low flow rate, it has been reported that large particles (i.e., $d = 60$ μm) cause a peak distortion and sample loss in the reduced channel [26].

Another important point is the slope of the calibration curve, the diameter-based selectivity, S_d, which has been found to be 0.7–0.8 as described earlier. For a considerable range of field strengths, the calibration curves are found to be nearly parallel to each other for some fixed flow rate [2, 23, 26]. The slope of calibration curve, and hence S_d, tends to increase when the spin rate is relatively low compared to the flow velocity employed for separation. For instance, the slope of calibration curve is found to be maintained about 0.7–0.8 between 800 and 1900 rpm at a typical flow rate ($\dot{V} = 6.0$ mL/min) used in earlier works [23, 24, 26]. When the spin rate

is lowered to 600 rpm at the same flow rate, the slope S_d appears to be as large as 0.92. However, at a higher flow rate of 10 mL/min, the abnormal increase in the slope appears up to 1100 rpm [27]. This is due to the early elution of large particles with regard to the hyperlayer operation as in flow FFF. In this case, the increase in selectivity does not accompany the substantial increase in the separation efficiency, since resolution in the separation of large particles is poorer than in typical calibration runs. It should be noted that the flow rate influences the optimum range of field strength which maintains the parallel relationship, and therefore constant S_d.

While the theory and empirical confirmation of calibration procedure in Sd/StFFF have been described in earlier publications, an optimum calibration run is often difficult to select in practice, because particulate materials in nature are so diverse in size range and shape. The calibration procedure described in this review is strictly applicable only to spherical particles. The effect of particle shape on retention in Sd/StFFF is not clearly understood, because the role of the hydrodynamic lift forces acting on irregularly shaped particles is somewhat more complicated than for spherical particles. The known phenomenon of these particles thus far is that irregular particles migrate at higher positions above the wall than would be expected according to the apparent size, and the degree of shift in retention is also dependent on the shape. However, for particles of nearly spherical or blocky shape, this deviation is not as serious as in a plate and rod shape, but results in a slight uncertainty in the particle size distribution obtained. A proper methodology must be established to incorporate all of these factors, including the sliding or tumbling motion of irregular particles that can be expected in lamina flowstreams of an FFF channel.

REFERENCES

1. J.C. Giddings, *Science* **260,** 1456 (1993).
2. J.C. Giddings, M.H. Moon, P.S. Williams, and M.N. Myers, *Anal. Chem*. **63,** 1366 (1991).
3. J.C. Giddings, S.K. Ratanathanawongs, and M.H. Moon, *KONA*: *Powder Particle* **9,** 200 (1991).
4. M.H. Moon and J.C. Giddings, *Anal. Chem*. **64,** 3029 (1992).
5. P.S. Williams, M.H. Moon, and J.C. Giddings, in *Particle Size Analysis*, N.G. Stanley-Wood and R.W. Lines, Eds. (Royal Society of Chemistry, Cambridge, UK), 1992.
6. J.C. Giddings, M.N. Myers, M.H. Moon, and B.N. Barman, in *Particle Size Distribution*, T. Provder, Ed., ACS Symposium Series no. 472 (ACS, Washington, DC, 1991), Chapter 13.
7. J.C. Giddings, *Chem. Eng. News* **66,** 34 (1988).
8. K.D. Caldwell, *Anal. Chem*. **60,** 959A (1988).
9. B.N. Barman and J.C. Giddings, *Langmuir* **8,** 51 (1992).
10. J.C. Giddings, S.K. Ratanathanawongs, B.N. Barman, M.H. Moon, G. Liu, B.L. Tjelta, and M.E. Hansen, in *Colloid Chemistry of Silica*, H. Bergna, Ed., Advances in Chemistry Series no. 234 (ACS, Washington, DC, 1993).
11. R. Beckett, G. Nicholson, B.T. Hart, M. Hansen, and J.C. Giddings, *Water Res*. **22,** 1535 (1988).
12. S. Levin and E. Klausner, *Pharm. Res*. **12,** 1218 (1995).
13. J.T. Li and K.D. Caldwell, *Langmuir* **7,** 2034 (1991).
14. K.D. Caldwell, J. Li, J.-T. Li, and D.G. Dalgleish, *J. Chromatogr*. **604,** 63 (1992).
15. R.A. Arlauskas and J.G. Weers, *Langmuir* **12,** 994 (1986).
16. T. Koch and J.C. Giddings, *Anal. Chem*. **58,** 994 (1986).
17. K.D. Caldwell, T.T. Nguyen, M.N. Myers, and J.C. Giddings, *Sep. Sci. Technol*. **14,** 935 (1979).
18. P.S. Williams, T. Koch, and J.C. Giddings, *Chem. Eng. Commun*. **111,** 121 (1992).
19. P.S. Williams, S. Lee, and J.C. Giddings, *Chem. Eng. Commun*. **130,** 143 (1994).
20. P.S. Williams, M.H. Moon, Y. Xu, and J.C. Giddings, *Chem. Eng. Sci*. **51,** 4477 (1996).
21. P.S. Williams, M.H. Moon, and J.C. Giddings, *Colloids Surf. A* **113,** 215 (1996).
22. R.E. Peterson II, M.N. Myers, and J.C. Giddings, *Sep. Sci. Technol*. **19,** 307 (1984).
23. J.C. Giddings and M.H. Moon, *Anal. Chem*. **63,** 2869 (1991).
24. M.H. Moon and J.C. Giddings, *J. Food Sci*. **58,** 1166 (1993).
25. R. Beckett, Y. Jiang, G. Liu, M.H. Moon, and J.C. Giddings, *Part Sci. Technol*. **12,** 89 (1994).
26. M.H. Moon and J.C. Giddings, *Ind. Eng. Chem. Res*. **35,** 1072 (1996).
27. M.H. Moon, Ph.D. dissertation, University of Utah, 1991.